The Use of Reflection from Vegetation for Estimating Broken-Cloud Optical Depth

W. J. Wiscombe and A. Marshak
National Aeronautics and Space Administration
Goddard Space Flight Center
Climate and Radiation Branch
Greenbelt, Maryland

Y. Knyazikhin
Boston University
Department of Geography
Boston, Massachusetts

A. B. Davis
Los Alamos National Laboratory
Space and Remote Sensing Sciences Group
Los Alamos, New Mexico

Introduction

The objectives of our study are to exploit the sharp spectral contrast in vegetated surface reflectance across 0.7-µm wavelength (e.g., Tucker 1979) to retrieve cloud properties from ground-based radiance measurements. Based on this idea, we have developed a new technique to retrieve cloud optical depth in the simultaneous presence of broken clouds and green vegetation (Figure 1), using ground zenith radiance measurements in two narrow spectral bands on each side of the step-function in vegetation albedo near 0.7 µm. Below 0.7 µm in the visible (VIS) spectral region, the chlorophyll in green vegetation absorbs 90% to 95% of solar radiation; thus its albedo is low. In contrast, above 0.7 µm in the near infrared (NIR) spectral region, the green vegetation reflects 45% to 50%, and its albedo is high. As a result, in the NIR region the green vegetation acts as a powerful reflector illuminating horizontally inhomogeneous clouds from below. This provides the extra information needed to largely remove the ambiguity in measured downwelling radiance caused by radiative effects of the three-dimensional (3D) cloud structure.

Three Main Atmospheric Cases

For proof-of-concept measurements, we deployed a modified CIMEL multi-channel sunphotometer on the roof of Building 33 at the National Aeronautics and Space Administration's (NASA's) Goddard Space Flight Center (GSFC). The modified CIMEL measures radiance with 20-sec. temporal resolution. It has a narrow field of view of 1° and four filters at 0.44 µm, 0.67 µm, 0.87 µm, and 1.02 µm designed for the retrieval of aerosol properties in clear-sky conditions.

Figure 1. Clouds over the Snake River in Idaho, courtesy of the multi-angle imaging spectroradiometer (MISR) Web Site. Note the inhomogeneity of the surface.

Figure 2 shows a 22-min fragment of zenith radiance measured by a ground-based CIMEL pointed straight up.

There are three distinct regions in Figure 2: (from left to right) a single unbroken cloud, broken clouds, and a clear sky. For clear-sky conditions, because of Rayleigh scattering and optically thicker aerosol at smaller wavelengths, zenith radiance increases from 1.02 μm to 0.44 μm. By contrast, for cloudy conditions, radiances in channels 0.44 μm and 0.67 μm are almost indistinguishable; this is also true for channels 0.87 μm and 1.02 μm. This is a clear indication that in the presence of clouds, the spectral contrast in surface albedo dominates over Rayleigh and aerosol effects. In contrast to the small fluctuations typical for clear and even cloudy skies, broken clouds show sharp changes in radiances around cloud edges.
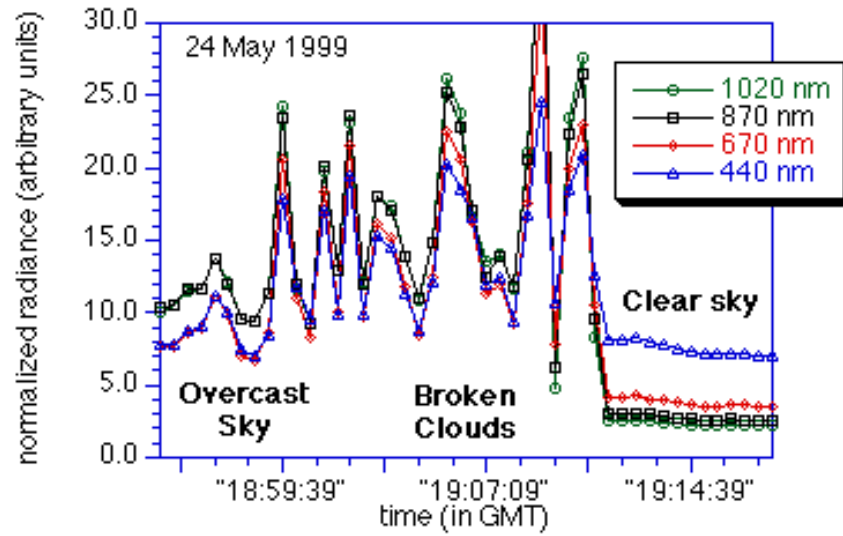
Figure 2. Zenith radiance measured by a CIMEL photometer on the roof of Building 33 at NASA GSFC on May 24, 1999. Four channels are used: 0.44 μm, 0.67 μm, 0.87 μm, and 1.02 μm. The measured radiance is normalized by the solar flux at the top of the atmosphere (TOA) in the corresponding spectral interval.

To be more formal, based on photon cloud-vegetation interactions, we will distinguish three main cases:

1) Atmosphere dominates (Figure 3a). In this case

$$I_{440} > I_{670} > I_{870} > I_{1020} \tag{1}$$

and aerosol optical properties can be retrieved.

2) (Green) surface and cloud dominates (Figure 3b). In this case

$$I_{440} \approx I_{670} < I_{870} \approx I_{1020} \tag{2}$$

and cloud optical properties can be retrieved (provided we know the surface albedo).

3) Transition between the first two cases (Figure 3c), characterized by rapid changes between the "order" of I_λ from cloudy to clear and back. In this case, neither aerosol nor cloud properties can be reliably retrieved using only one wavelength.
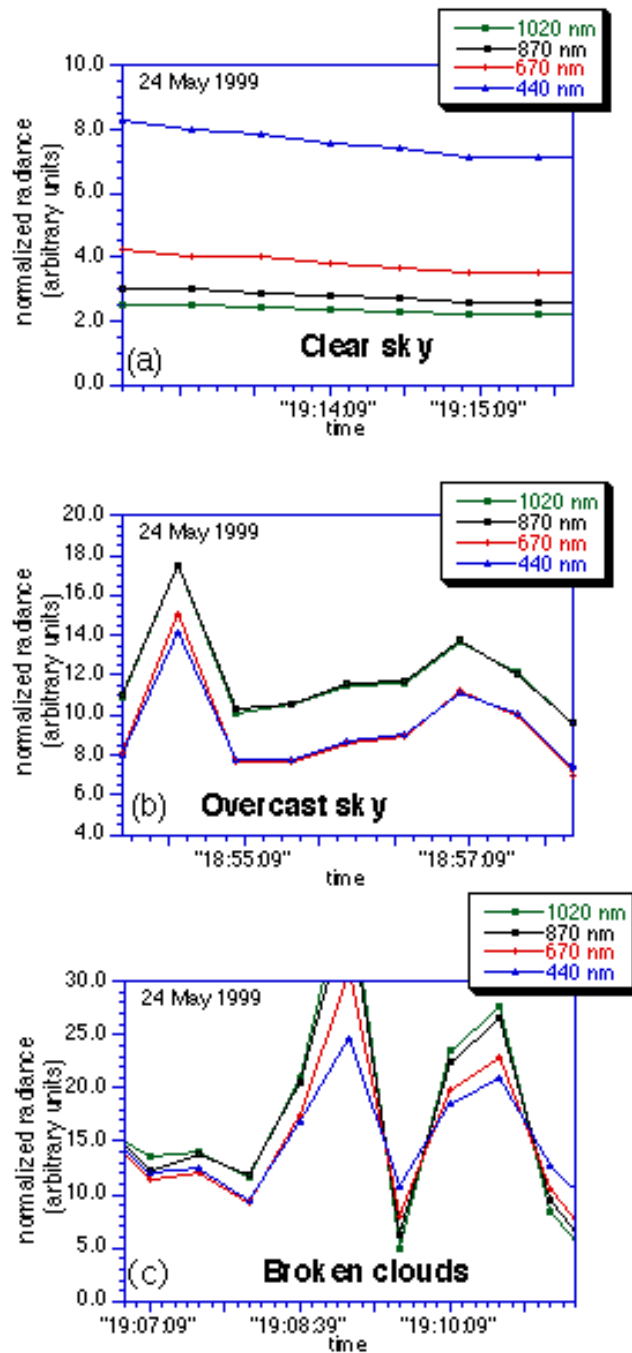
Figure 3. Fragments from Figure 2: (a) Clear sky, (b) overcast sky, and (c) broken clouds.

By analogy with the Normalized Difference Vegetation Index (NDVI, Tucker 1979), we define the Normalized Difference Cloud Index (NDCI) as a ratio between the difference and the sum of two normalized (by the solar flux at the TOA) zenith radiances measured for two narrow spectral bands in the NIR and VIS spectral regions (Marshak et al. 2000),

$$NDCI = \frac{I_{NIR} - I_{VIS}}{I_{NIR} + I_{VIS}} \qquad (3)$$

From Eqs. (1) and (2), the NDCI will be negative for a clear sky and positive for an overcast sky (Figure 4). In case of broken clouds, the NDCI can be either positive or negative depending on whether there is a cloud in the zenith direction or not.

We claim that for intervals of NDCI > 0, the fluctuations of NDCI correspond to natural fluctuations of cloud optical depth and are much less influenced by 3D radiative effects than any single-channel measurement.
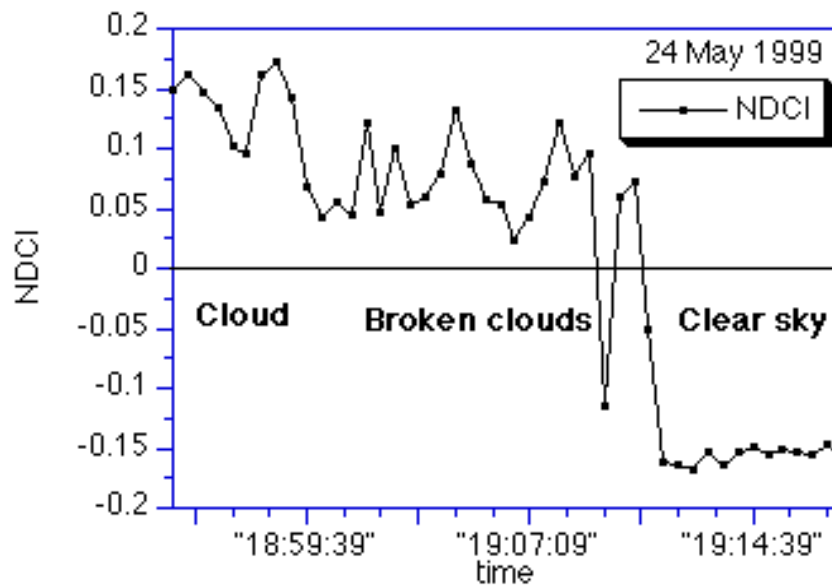

Figure 4. The NDCI defined in Eq. (3) for 0.65 μm and 0.87 μm and corresponding to the measurements in Figure 2.

1D and 3D Radiative Transfer

In this section, we first show that, in plane-parallel geometry, in contrast to zenith radiance, the NDCI is a monotonic function with respect to cloud optical depth. Then we focus on 3D radiative transfer and show how the NDCI can be used to retrieve cloud optical depth even in the case of broken clouds.

1D Calculations

Figure 5 shows plane-parallel calculations of NDCI with respect to cloud optical depth. In contrast to either zenith radiance in VIS or NIR, each value of NDCI corresponds to one and only one optical depth. But one drawback is that, for large τ, in general, the derivatives,

$$0 < \frac{d(\text{NDCI})}{d\tau} < \left| \frac{dI_\lambda}{d\tau} \right|. \tag{4}$$

This means that the retrieval of cloud optical depth is more sensitive to small changes in the NDCI radiance.
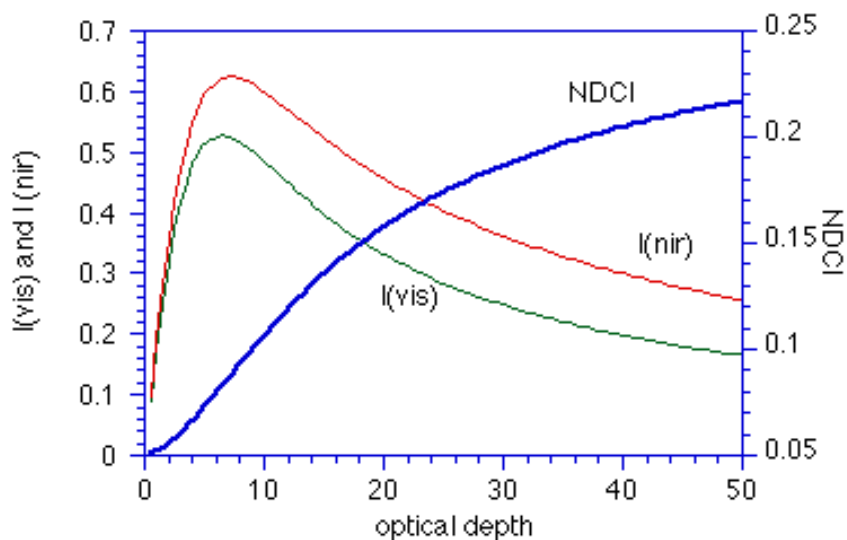

Figure 5. Plane-parallel radiative transfer. Solar zenith angle is 60°.

3D Calculations and Optical Depth Retrieval

In addition to a two-valued 1D zenith radiance vs. optical depth (Figure 5), 3D radiative effects, such as "smoothing" by multiple scattering and "roughening" by cloud edges (Marshak et al. 2000), prevent a one-to-one relationship between cloud optical depth and zenith radiances. This makes it absolutely impossible to retrieve cloud optical thickness on a pixel-by-pixel basis, at least for optical depths between 5 and 15 (Figure 6).

In Figure 6, for black surface (VIS), the 3D results are scattered around a theoretical 1D curve, while for bright surfaces (NIR), 1D radiance systematically underestimates 3D radiances for large optical depths. This is understandable since for 3D clouds, more radiation is transmitted through; thus, more radiation is reflected back from thick clouds to the surface. Hence, for large τ, it would be naïve to expect a good 1D retrieval from the real measured NDCI (Figure 7).

However, the 1D retrieval of optical depth smaller than 20 is quite reasonable even in this very complex case of broken clouds and solar zenith angle of 60°. Figure 8 shows a 23-km fragment of cloud optical depth averaged over 0.4 km. The mean (absolute) difference between true and retrieved optical depth is 1.6 and the standard deviation is only 2.
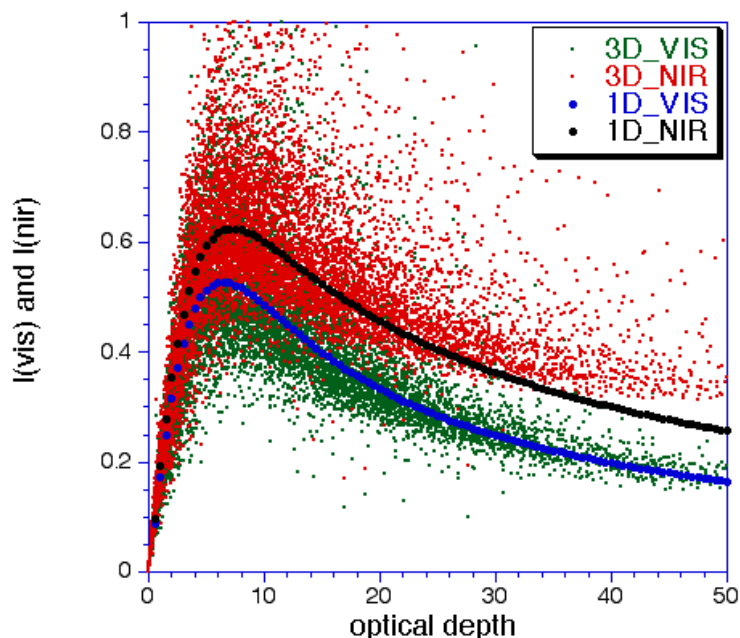
Figure 6. Downward radiances calculated by Monte Carlo methods for "black" surface (VIS, $\rho = 0.0$), and "bright" surface (NIR, $\rho = 0.5$). Pixel size is 25 m, solar zenith angle $\theta_0 = 60°$, $\varpi_0 = 1.0$, Henyey-Greenstein scattering phase function. Horizontal distribution of cloud optical depth is simulated by a 10-steps bounded cascade model (Cahalan 1994) with parameters $\langle \tau \rangle = 13$, $\beta = 1.4$ and $\rho = 0.35$. Geometrical cloud thickness is 300 m; cloud base height is 1 km. Holes are added as in Marshak et al. (1998). The results of 1D radiative transfer calculations from Figure 5 are added for convenience.
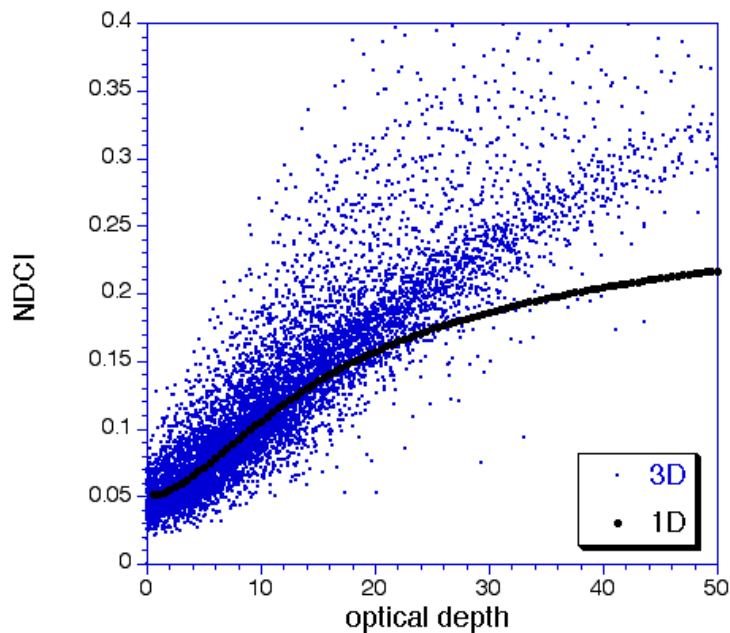

Figure 7. The same as in Figure 6 but for the NDCI defined by Eq. (3).
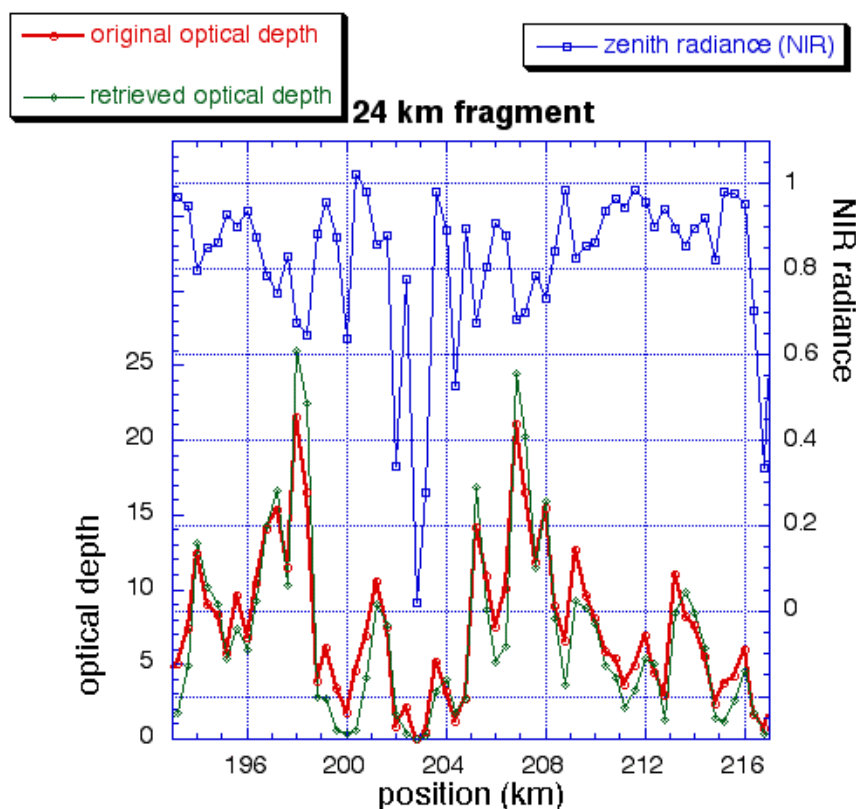
Figure 8. A 24-km fragment of the original optical depth and the retrieved one from the NDCI using Figure 5. Zenith radiance indicates a multi-valued character of the problem; e.g., radiances around 198 km, 200 km, 205 km, 208 km, and 216 km are 0.68±0.2 but correspond to completely different values of optical depth.

Measurements of Flux NDCI at the CART Site in Oklahoma

Flux NDCI and LWP

We used downwelling flux at the surface measured by the shortwave spectrometer (SWS) at the Atmospheric Radiation Measurement (ARM) site in Oklahoma. SWS measures solar spectral flux between 0.35 μm and 2.5 μm, continuously, with spectral resolution 1 nm and temporal resolution of less than 1 min. In addition to SWS, we also used the microwave water radiometer (MWR) that measures column-integrated liquid water (LWP).

Figure 9 shows a ratio between the difference and the sum of two downwelling fluxes (per unit incident flux) measured by SWS at 0.67 μm and 0.87 μm on April 29, 1998. Single and multilayered boundary layer clouds were reported that day. We plotted the ratio (flux NDCI) on the same plot as cloud liquid water path (LWP) averaged over 1 min. Clearly, flux NDCI is highly correlated with LWP. It is expected, though, that the correlation between NDCI and LWP will be even better if radiances are used instead of fluxes.
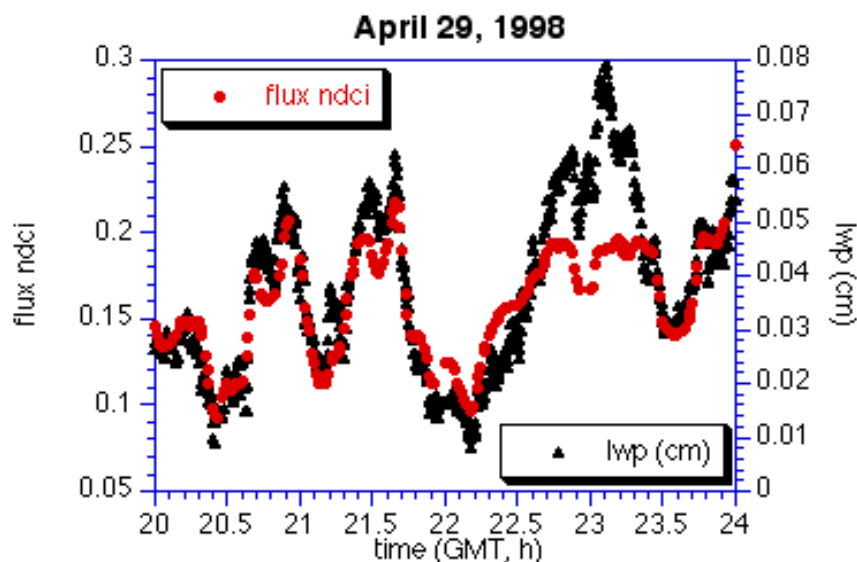
Figure 9. Flux NDCI and cloud LWP measured at the ARM site in Oklahoma and averaged over 1 min. Note a poor correlation for about 40 min from 22.7 h to 23.3 h. The reason has not yet been completely understood. We believe that having radiances instead of fluxes will improve this correlation.

Inhomogeneity of Surface Reflectance

Surface reflectance at the ARM site in Oklahoma is very inhomogeneous (Figure 10). However, this does not prevent the use of NDCI because the contribution from surface is integrated over several km (depending on cloud base height) and the local surface properties are less important than its average characteristics (Knyazikhin and Marshak 2000). Figure 11 shows nadir reflectivity around the ARM site in Oklahoma averaged over scales from 30 m to 5 km. It is clear that in spite of strong surface inhomogeneity, the value of surface reflectivity stabilizes after averaging over 1 km - 1.5 km for both VIS and NIR spectral regions.

Conclusion

The main ideas of the proposed method are as follows:

- use two wavelengths to create an NDVI-like index, that we call "NDCI" (for normalized difference cloud index). One wavelength is in VIS where vegetation albedo is low, and another wavelength is in NIR where vegetation albedo is high.

- use radiance instead of flux

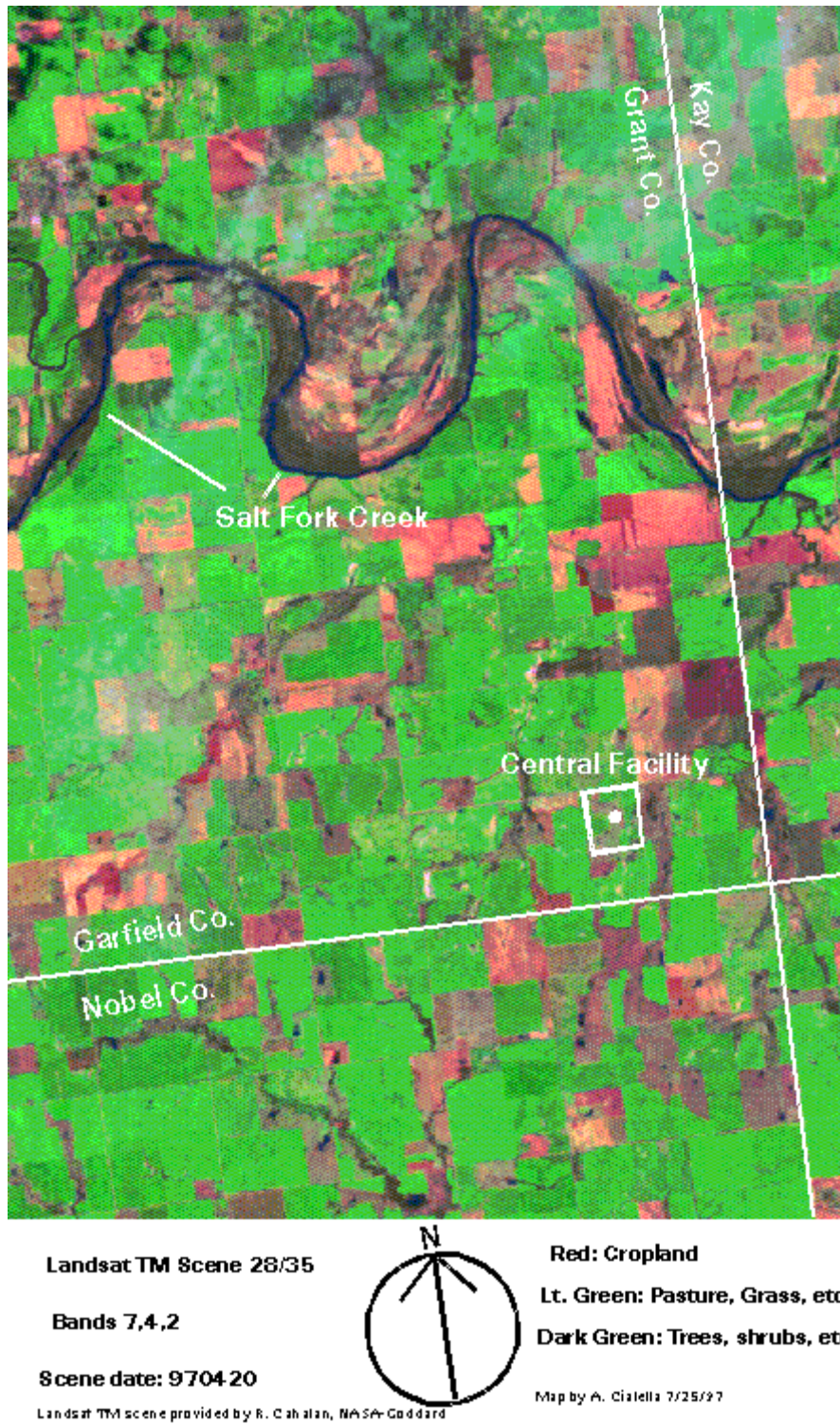- retrieve broken-cloud optical depth from this index using 1D radiative transfer.

Figure 10. A Landsat TM Scene of the ARM Oklahoma site taken on April 20, 1997. Bands 2, 4, and 7 have been used.
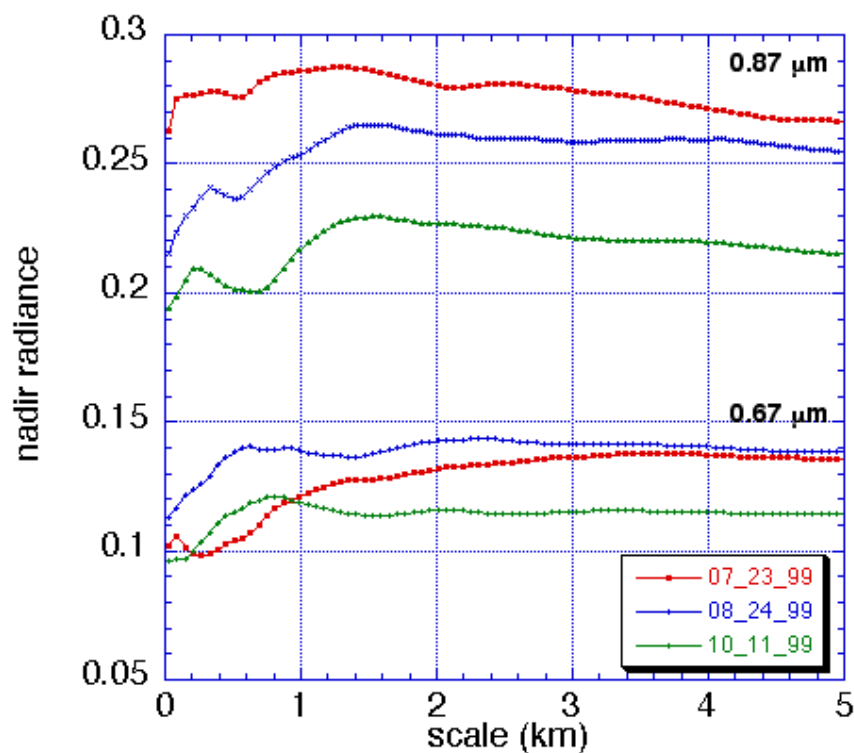
Figure 11. Dependence of average nadir radiance around the ARM site in Oklahoma on the averaging scale. The data are taken from the three Landsat scenes measured on July 23, August 24, and October 11, 1999. (Courtesy of G. Wen, Joint Center for Earth, Systems, and Technology, University of Maryland, Baltimore County).

The preliminary results look very promising, both theoretically and from measurements made with the CIMEL at NASA/GSFC and the shortwave spectrometer from the ARM site in Oklahoma. We showed that this technique can get results where monochromatic methods fail. A good correlation with liquid water path suggests using the NDCI even for extending our ability to get droplet effective radius.

Corresponding Author

A. Marshak, 301-614-6122, marshak@climate.gsfc.nasa.gov

References

Cahalan, R. F., 1994: Bounded cascade clouds: Albedo and effective thickness. *Nonlinear Processes in Geoph.*, **1**, 156-167.

Knyazikhin, Y., and A. Marshak, 2000. Mathematical aspects of BRDF modeling: Adjoint problem and Green's function. *Remote Sens. Reviews*. In press.

Marshak, A., A. Davis, W. J. Wiscombe, W. Ridgway, and R. F. Cahalan, 1998: Biases in shortwave column absorption in the presence of fractal clouds. *J. Climate*, **11**, 431-446.

Marshak, A., Y. Knyazikhin, A. Davis, W. Wiscombe, and P. Pilewskie, 2000. Cloud-vegetation interaction: Use of normalized difference cloud index for estimation of cloud optical thickness. *Geoph. Res. Lett.* In press.

Tucker, C. J., 1979: Red and photographic infrared linear combination for monitoring vegetation. *Remote Sens. Environ.*, **8**, 127-150.